Interleukin-6 Causes Myocardial Failure and Skeletal Muscle Atrophy in Rats

Sofie P.M. Janssen; Ghislaine Gayan-Ramirez, PhD; An Van Den Bergh; Paul Herijgers, MD, PhD; Karen Maes; Erik Verbeken, MD, PhD; Marc Decramer, MD, PhD

Background—The impact of interleukin (IL)-6 on skeletal muscle function remains the subject of controversy.

Methods and Results—The effects of 7-day subcutaneous administration of recombinant human IL-6 were examined at 3 doses, 50, 100, or 250 $\mu g \cdot kg^{-1} \cdot d^{-1}$, in rats. Skeletal muscle mass decreased dose-dependently (with increasing dose: in the diaphragm, −10%, P=NS; −15%, P=0.0561; and −15% $P<0.05$; and in the gastrocnemius, −9%, P=NS; −9%, P=NS; and −18%, $P<0.005$) because of decreases in cross-sectional area of all fiber types without alterations in diaphragm contractile properties. Cardiovascular variables showed a dose-dependent heart dilatation (for end-diastolic volume: control, 78 μL; moderate dose, 123 μL; and high dose, 137 μL, $P<0.001$), reduced end-systolic pressure (control, 113 mm Hg; moderate dose, 87 mm Hg; and high dose, 90 mm Hg; $P=0.037$), and decreased myocardial contractility (for preload recruitable stroke work: control, 79 mm Hg; moderate dose, 67 mm Hg; and high dose, 48 mm Hg; $P<0.001$). Lung edema was confirmed by an increased wet-to-dry ratio (control, 4.2; moderate dose, 4.6; and high dose, 4.5; $P<0.001$) and microscopy findings. These cardiovascular alterations led to decreases in organ blood flow, particularly in the diaphragm (control, 0.56 $mL \cdot min^{-1} \cdot g^{-1}$; moderate dose, 0.21 $mL \cdot min^{-1} \cdot g^{-1}$; and high dose, 0.23 $mL \cdot min^{-1} \cdot g^{-1}$; $P=0.037$). In vitro recombinant human IL-6 administration did not cause any alterations in diaphragm force or endurance capacity.

Conclusions—IL-6 clearly caused ventilatory and peripheral skeletal muscle atrophy, even after short-term administration. Blood flow redistribution, resulting from the myocardial failure induced by IL-6, was likely responsible for this muscle atrophy, because IL-6 did not exert any direct effect on the diaphragm. **(*Circulation*. 2005;111:996-1005.)**

Key Words: interleukins ■ cardiomyopathy ■ blood flow ■ contractility ■ muscles

Serum levels of interleukin (IL)-6 are elevated in various conditions such as heart failure,[1] sepsis,[2] burns,[3] acute respiratory distress syndrome, pneumonia,[4] and exacerbations of chronic obstructive pulmonary disease,[5] in all of which clinically significant skeletal muscle weakness is known to be present.[6–11] However, whether this muscle weakness is caused by IL-6 remains unclear. Indeed, on one hand, IL-6–transgenic mice exhibited skeletal muscle atrophy,[12] which was fully reversed by administration of IL-6 receptor antagonists.[13] By contrast, IL-6 failed to augment muscle proteolysis in vitro[14] and even facilitated differentiation of cultured rat myoblasts.[15]

On the other hand, systolic ventricular dysfunction is known to induce selective diaphragm atrophy.[6] Hence, it appears possible that the aforementioned effects of IL-6 on skeletal muscle would be caused by an effect on the myocardium, because IL-6 or members of its family are known to induce ventricular hypertrophy and to reduce basic hemodynamic variables. Indeed, concentric hypertrophy and decreases in ventricular volume were observed in IL-6$^+$/IL-6 receptor$^+$–transgenic mice.[16] Moreover, in vivo administration of cardiotrophin-1, a cytokine belonging to the same family as IL-6, induced increases in ventricular-to-body weight ratio, associated with reduced mean arterial pressure and systemic vascular resistance.[17,18] Furthermore, the occurrence of morphological changes in the myocardium and decreased myocardial contractility are also well supported by several in vitro experiments after administration of the aforementioned cytokines. First, cardiotrophin-1 was shown to induce a clear hypertrophic response in neonatal rat cardiac myocytes.[19] Second, a direct negative inotropic effect on isolated hamster papillary muscle was exerted by IL-6, likely related to upregulation of myocardial nitric oxide synthase.[20] In addition, IL-6 was shown to downregulate sarcoplasmic reticulum Ca^{2+} ATPase (SERCA2) activity in isolated rat cardiac myocytes.[21] Finally, administration of IL-6 to rat

Received June 21, 2004; revision received October 7, 2004; accepted November 12, 2004.

From the Laboratory of Pneumology (S.P.M.J., G.G.-R., K.M., M.D.), Respiratory Muscle Research Unit; the Center for Experimental Surgery and Anesthesiology (A.V.D.B., P.H.), Cardiovascular Research Unit; and the Department of Pathology (E.V.), Katholieke Universiteit Leuven, Leuven, Belgium.

The online-only Data Supplement can be found with this article at http://www.circulationaha.org.

Reprint requests to Prof Marc Decramer, MD, PhD, Respiratory Division, University Hospital Gasthuisberg, Herestraat 49, B-3000 Leuven, Belgium. E-mail Marc.Decramer@uz.kuleuven.ac.be

Circulation **is available at http://www.circulationaha.org** **DOI: 10.1161/01.CIR.0000156469.96135.0D**

cardiac myocyte cultures resulted in reduced expression of α-myosin heavy chain (MHC), β-myosin heavy chain, and cardiac α-actin.[22] The present study was designed to reconcile the aforementioned observations by determining whether IL-6 causes myocardial dysfunction, leading to skeletal muscle atrophy.

Methods

A detailed version of this section is available in the online-only Data Supplement.

Experimental Protocol

The ethics committee of the medical faculty of the Katholieke Universiteit Leuven, Leuven, Belgium, approved the present study. Six series of experiments were conducted on 139 male Wistar rats, 8 to 10 weeks old and weighing 350 to 450 g. In the first series, 16 rats received a 7-day continuous infusions of a low (50 $\mu g \cdot kg^{-1} \cdot d^{-1}$, n=8) or moderate (100 $\mu g \cdot kg^{-1} \cdot d^{-1}$, n=8) dose of recombinant human (rh) IL-6. Eight control rats received phosphate-buffered saline (PBS) infusions. In a second series, 15 rats received a high dose (250 $\mu g \cdot kg^{-1} \cdot d^{-1}$, n=9) of rhIL-6 or PBS (control, n=6). In both experiments, body and tissue mass, diaphragm in vitro contractile properties, and morphometry of the diaphragm and gastrocnemius were performed.

In a third series of experiments, hemodynamic measurements were performed in 31 rats combined either with determination of body and tissue mass, lung histology and water content, and blood sampling (control, n=4; 100 $\mu g \cdot kg^{-1} \cdot d^{-1}$ rhIL-6, n=8; or 250 $\mu g \cdot kg^{-1} \cdot d^{-1}$ rhIL-6, n=5) or with examination of heart histology (control, n=4; 100 $\mu g \cdot kg^{-1} \cdot d^{-1}$ rhIL-6, n=6; or 250 $\mu g \cdot kg^{-1} \cdot d^{-1}$ rhIL-6, n=4).

In a fourth series, organ and muscle blood flows were assessed with the use of colored microspheres in 17 rats (control, n=4; 100 $\mu g \cdot kg^{-1} \cdot d^{-1}$ rhIL-6, n=6; or 250 $\mu g \cdot kg^{-1} \cdot d^{-1}$ rhIL-6, n=7). In a fifth series, food intake was measured in 24 rats (control, 100 $\mu g \cdot kg^{-1} \cdot d^{-1}$ rhIL-6, and 250 $\mu g \cdot kg^{-1} \cdot d^{-1}$ rhIL-6; n=8 per group), whereas 18 rats were used to assess activity levels (control, 100 $\mu g \cdot kg^{-1} \cdot d^{-1}$ rhIL-6, and 250 $\mu g \cdot kg^{-1} \cdot d^{-1}$ rhIL-6; n=6 per group). Serum rhIL-6 and endogenous rat IL-6 were measured in the moderate- and high-dose groups of the third and fifth experimental series. Finally, in a sixth series, diaphragm force was assessed in vitro by adding rhIL-6 or Krebs' solution to the tissue bath (n=5 per group).

Pump Implantation

Rats were anesthetized intraperitoneally with sodium pentobarbital (60 mg/kg; Nembutal, Sanofi). Subsequently, Alzet miniosmotic pumps (model 2001, Iffa Credo) were implanted subcutaneously. Pumps implanted in experimental animals were filled with sterile PBS (Cambrex Bio Science Verviers), rhIL-6, and rat serum (1%, vol/vol). Control rats received an identical volume of PBS, human albumin (0.1% wt/vol; ICN Biomedicals, Inc), and rat serum.

Diaphragm In Vitro Contractile Properties

Animals were anesthetized intraperitoneally with sodium pentobarbital, tracheotomized (14-gauge Insyte catheter, BD), and ventilated at a constant rate of 60 cycles/min (Harvard Apparatus Co). Subsequently, 2 small strips of both costal diaphragm regions were dissected and placed at their optimal length. Contractile properties were further studied at 37°C.[23,24] The whole diaphragm, heart, right scalenus medius, gastrocnemius, soleus, extensor digitorum longus, and plantaris muscles were weighed after being trimmed and dried in the first experiment. Similar measurements were performed in the second and third experiments, together with the weighing of lung and liver.

Morphometry of the Diaphragm and Gastrocnemius

Gastrocnemius and costal diaphragm samples were frozen in isopentane cooled with LN_2.[23] Serial 10-μm cross sections were then stained for myofibrillar ATPase at pH 4.3 or 4.5 to identify the different fiber types.[25] Morphometric examination was carried out microscopically (Leitz Laborlux S) at ×20 magnification with a digital video camera (model VC-2512, Sanyo B/W CCD camera) connected to a computerized image analysis system (Quantimet 500, Leica, Cambridge Ltd) to determine fiber diameter, fiber proportion, cross-sectional area (CSA), and residual interstitial area.[23]

Diaphragm In Vitro IL-6 Administration

Contractile properties and endurance of untreated diaphragm strips were studied at 37°C[23,24] after 30 minutes' incubation in Krebs' solution containing 12 ng rhIL-6/mL or Krebs' solution alone.

Cardiovascular Functional Parameters

Rats were anesthetized intraperitoneally with urethane (600 mg/kg) and α-chloralose (160 mg/kg), tracheotomized, and ventilated with a pressure-controlled respirator (end-inspiratory pressure, 12 mm Hg; end-expiratory pressure, 2 mm Hg; Hugo Sachs Elektronik). The right carotid artery was exposed, and a microtip pressure-conductance combination catheter (SPR-847 catheter connected to an ARIA-1 setup, Millar Instruments) was advanced into the left ventricle to measure basal hemodynamic parameters by generating pressure-volume loops. Contractility parameters were obtained by decreasing left ventricular preload, performed by temporary occlusion of the inferior vena cava. Volume calibrations of the measured conductance were performed at the end of each experiment with known blood volume.

Heart Histology

A winged needle (21-gauge, BD Valu-Set) was inserted into the left ventricle. Simultaneously a small hole was made in the right atrium, and 2 mL of 0.1 mol/L cadmium chloride was injected into the left ventricle to arrest the heart in dilatation. After perfusion with 0.9% NaCl, fixation was performed with 4% formaldehyde. Excised hearts were then divided in 4 transverse slices and embedded in paraffin. Serial 7-μm slices were stained with hematoxylin and eosin (H&E). The right ventricular cavity was measured by using a microscope digital video camera connected to a computerized image analysis system. Values were expressed as a percentage of total heart surface area limited by the outer margin of the ventricular wall.

Blood Flow Measurements

Anesthesia and tracheotomy were performed in the same way as for the hemodynamic measurements. Subsequently, 2 PE50 catheters (Intramedic, Clay Adams) were inserted into the left ventricle and femoral artery to determine blood flow of the right and left ventricles, diaphragm, right gastrocnemius, right and left kidneys, spleen, jejunum, and colon by injecting 15-μm yellow microspheres into the left ventricle (400 μL; Dye-Trak, Triton Technology).[26] Simultaneously, heart rate and arterial and ventricular pressures were recorded. Blood flow was divided by tissue weight and expressed as milliliters per minute per gram wet weight.

Lung Histology and Water Content

Left lungs were fixed in 4% formaldehyde. Subsequently, 5-μm paraffin slices were stained with H&E and examined by a pathologist. The right lobes were used to determine water content by measuring wet-to-dry ratio after desiccation for 3 days at 80°C.

Serum Levels

Blood was sampled after cleavage of the vena cava and collected in EDTA tubes (BD Vacutainer systems). Serum rhIL-6 and rat IL-6 were measured by sandwich ELISA (IL-6 Flexia kit: sensitivity 3 pg/mL; rat IL-6 ELISA kit: sensitivity <8 pg/mL; Biosource Europe).

Food Intake

Free-fed animals were individually housed in metabolic cages at 23°C with a 14-hour light/10-hour dark cycle. Ad libitum food intake and body mass were recorded daily. Water was available ad libitum.

TABLE 1. Body and Organ Weights

	Control	Low	Moderate	High
Body weight, g				
At beginning of experiment 1	369±20	383±20	376±12	
At beginning of experiment 2	400±14			401±7
At end of experiment 1	367±21	370±31	361±13	
At end of experiment 2	417±18			382±8§
Weight of respiratory muscles, g				
Diaphragm, experiment 1	0.552±0.080	0.498±0.075	0.468±0.034*	
Diaphragm, experiment 2	0.600±0.056			0.510±0.047†
Scalenus medius, experiment 1	0.482±0.035	0.478±0.080	0.458±0.046	
Scalenus medius, experiment 2	0.630±0.098			0.540±0.063†
Weight of peripheral muscles, g				
Gastrocnemius, experiment 1	1.829±0.242	1.673±0.338	1.673±0.114	
Gastrocnemius, experiment 2	2.170±0.133			1.770±0.107§
Soleus, experiment 1	0.143±0.015	0.154±0.014	0.143±0.010	
Soleus, experiment 2	0.211±0.018			0.183±0.024†
Plantaris, experiment 1	0.355±0.041	0.355±0.032	0.329±0.030	
Plantaris, experiment 2	0.414±0.030			0.350±0.029§
EDL, experiment 1	0.155±0.012	0.158±0.014	0.145±0.011	
EDL, experiment 2	0.193±0.019			0.168±0.011‡
Organ weight, g				
Heart, experiment 1	0.857±0.052	0.901±0.039	0.934±0.045†	
Heart, experiment 2	1.170±0.056			1.100±0.108
Liver, experiment 3	14.69±0.05		13.48±1.35	15.65±1.47

EDL indicates extensor digitorum longus.
Gabriel post hoc test: *P=0.056, †P<0.05, ‡P<0.01, §P<0.005 vs control.

Activity Level

Behavioral responses were tested for 16 hours on day 7 (8 hours under light conditions and 8 hours in the dark) with an infrared camera (Agema Thermovision 570) coupled to a digitizer board. Animals were represented by bright points on a dark background from which movements consequently could be deduced.[27] Values were expressed as centimeters of displacement per hour.

Statistics

Hemodynamics and blood flow variables were analyzed with Statistica 6 software. All other statistical analyses were performed with SAS version 6.12 (SAS Institute Inc). Data from 2 different diaphragm strips obtained from each rat were averaged. Differences between means of rats treated with rhIL-6 and control rats were assessed with a 1-way ANOVA or Kruskal-Wallis test for the first, third, fourth, and fifth experiments (with appropriate Gabriel, Scheffé, or Fisher post hoc comparison) or a Wilcoxon or unpaired t test for the second and sixth experiments. Pearson's correlation analysis was performed to assess relationships. A 2-sided probability value <0.05 was considered significant. Data are expressed as mean±SD.

Results

Body and Organ Weights

Body weight (Table 1) was similar between controls and experimental groups at the time of pump implantation. Only for the high-dose rhIL-6 group did body weight decrease significantly, by 8%, at the time of dissection (P<0.005). The low rhIL-6 dose had no effect on tissue weights. In rats treated with the moderate rhIL-6 dose, only diaphragm weight tended to decrease by 15% (P=0.0561). Heart weight increased significantly by 9% (P<0.05). For rats treated with the high rhIL-6 dose, the mass of all muscles studied decreased significantly by ≈15% (P<0.05).

Diaphragm In Vitro Contractile Properties

Twitch (P_t) and tetanic (P_o) tension were similar among all groups (pooled values of 465±84 and 2407±418 g/cm^2, respectively), although P_t/P_o decreased significantly in the high-dose group (0.196±0.007 versus 0.209±0.013 in control rats, P<0.05). Time to peak tension was identical in all groups (pooled value of 20±2 ms), whereas half-maximal relaxation time tended to decrease in the high-dose group (22±3 versus 23±3 ms in controls, P=0.0584). In the force-frequency curve, diaphragm force was comparable in all groups (Figure 1, upper panel). Furthermore, during the low-frequency fatigue run, no differences in force decline (pooled values of 56±5%; Figure 1, lower panel) were observed among the different groups.

Morphometry

Fiber proportion and residual interstitial area remained unchanged in both the diaphragm and gastrocnemius at all doses. Also, no changes in fiber dimensions were observed in the low- and moderate-dose groups. In the high-dose group, the diameter of all fiber types of the diaphragm decreased significantly, by ≈14%, compared with controls (type I,

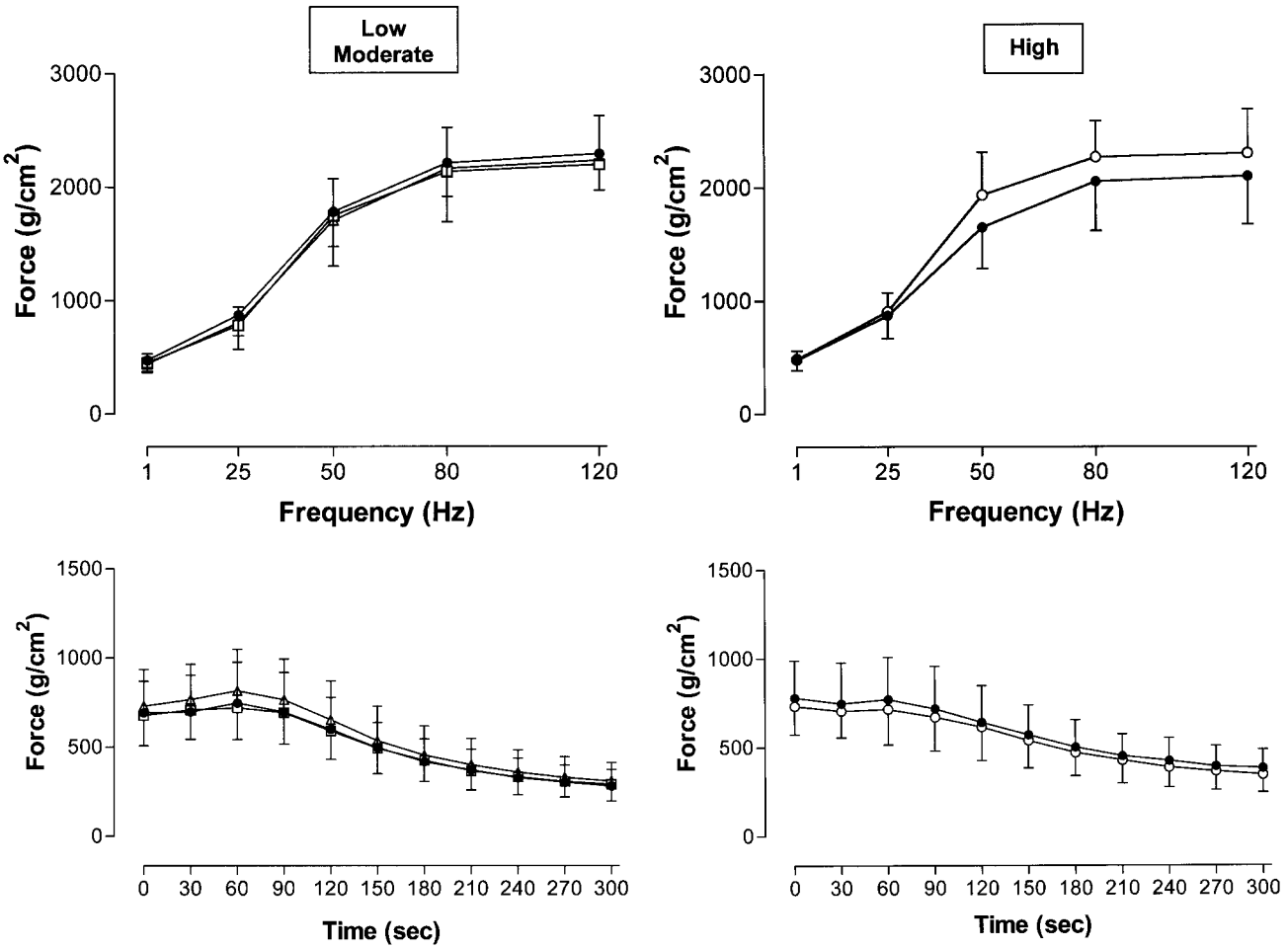

Figure 1. Diaphragm force-frequency (top) and endurance (bottom) data in low- (open squares), moderate- (open triangles), and high- (open circles) dose groups of animals compared with controls (solid circles). Force is expressed in g/cm^2; frequency in Hz.

30±3 versus 35±4 μm; type IIa, 35±1 versus 40±4 μm; and type IIx/b, 49±4 versus 58±7 μm; all $P<0.05$). The CSA of type IIa fibers decreased significantly by 19% (799±93 versus 987±158 μm^2 in control rats, $P<0.01$), whereas that of type IIx/b and type I fibers tended to decrease by 24% (1587±302 versus 2078±518 μm^2 in controls, $P=0.0518$) and 17%, respectively (Figure 2).

The diameter of gastrocnemius internal fiber types I and IIx/b tended to decrease by 9% in the high-dose group (type I, 49±5 versus 54±2 μm in controls, $P=0.0731$; type IIx/b, 50±6 versus 55±3 μm in control rats; $P=0.0855$), whereas that of internal type IIa fibers remained unchanged. For the external part, type IIx/b diameter tended to decrease by 5% (60±2 versus 64.0±4 μm in control animals, $P=0.0747$). The CSA of fiber types I and IIa also tended to decrease by 15% and 14%, respectively (type I, 2184±384 versus 2575±283 μm^2 in control rats, $P=0.0677$; type IIa, 2036±371 versus 2384±170 μm^2 in controls, $P=0.0875$), whereas the CSA of both internal and external IIx/b fiber types did not change (Figure 3).

Diaphragm In Vitro IL-6 Administration

Addition of rhIL-6 to the tissue bath did not affect diaphragm P_t (366±75 versus 381±50 g/cm^2) or P_o (1965±457 versus 1975±165 g/cm^2), P_t/P_o (0.19±0.03 versus 0.19±0.01), time to peak tension (22.8±1.0 versus 20.8±1.5 ms), or half-maximal relaxation time (22.4±1.8 versus 27.2±5.0 ms) when compared with control strips. During determination of the force-frequency curve and the low-frequency fatigue run, generated forces were similar in both groups.

Cardiovascular Functional Parameters

End-diastolic volume ($P<0.005$) and stroke volume ($P<0.005$) under steady-state conditions increased significantly in a dose-dependent manner (Table 2), causing a remarkable shift to the right of the pressure-volume loops (Figure 4, upper panels). End-diastolic pressure was somewhat higher in the treated groups, but this difference failed to reach statistical significance. Heart rate, ejection fraction, maximal change of pressure over time (dP/dt), and τ, the time constant of relaxation, were not affected by treatment. End-systolic pressure ($P<0.05$) and arterial elastance ($P<0.001$) decreased significantly with both the moderate and high dose.

Preload recruitable stroke work and end-systolic elastance decreased significantly in a dose-dependent manner ($P<0.001$; Figure 4, lower panels). From these parameters, it is clear that despite the reduced contractility, cardiac output

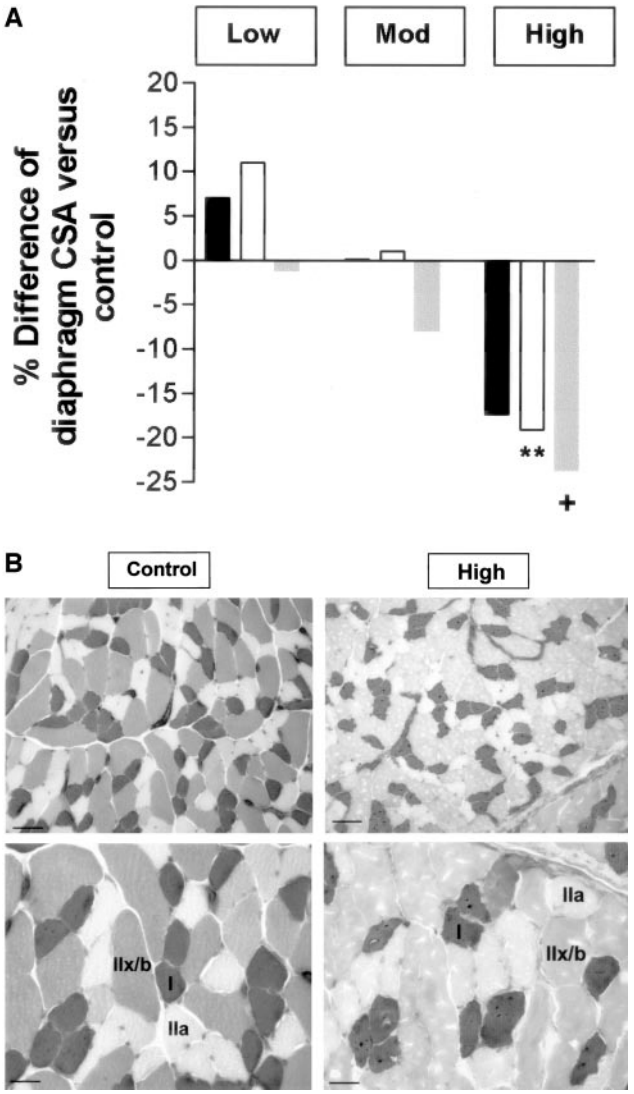

Figure 2. A, CSA of different fiber types (I, solid bars; IIa, open bars; IIx/b, gray bars) in diaphragm expressed as percentage difference from respective controls in rats treated with low (left), moderate (middle), or high (right) doses of rhIL-6. $^{**}P<0.01$, $+P=0.0518$. B, Representative diaphragm ATPase staining (pH 4.3) of control (left) and high-dose (right) rhIL-6 animal. Top panels correspond to ×200 magnification, bar=35 μm; bottom panels, to ×400 magnification, bar=17.5 μm. Note decreases in CSA of type IIa (white) and type IIx/b fibers (gray) in high-dose rhIL-6–treated animal. Abbreviations are as defined in text.

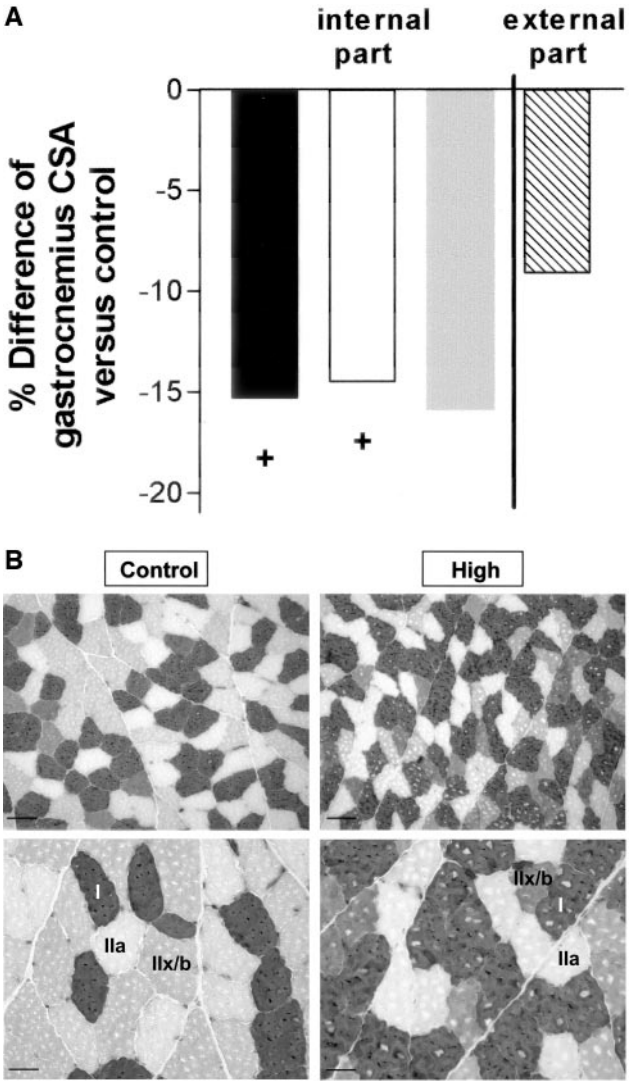

Figure 3. A, CSA of different fiber types (internal part: I, solid bar; IIa, open bar; IIx/b, gray bar; external part: IIx/b, hatched bar) in gastrocnemius expressed as percentage difference from respective controls in rats treated with high doses of rhIL-6. $+P<0.0875$. B, Representative gastrocnemius ATPase staining (pH 4.5, internal part) of control (left) and high-dose–treated (right) rhIL-6 animal. Top panels correspond to ×200 magnification, bar=35 μm; bottom panels, to ×400 magnification, bar=17.5 μm. Note decreases in CSA of type I fibers (black) and type IIa fibers (white) in high-dose rhIL-6–treated animal. Abbreviations are as defined in text.

($P<0.005$) increased because of larger stroke volumes combined with reduced afterload.

Correlations: Muscle Weight and Cardiovascular Functional Parameters

Positive correlations were found between diaphragm weight and end-systolic elastance, preload recruitable stroke work, and maximal elastance ($0.50<r<0.63$, $0.012<P<0.056$). Negative correlations were present between diaphragm weight and end-systolic volume, end-diastolic volume, and stroke work ($-0.62<r<-0.51$, $0.013<P<0.052$). All other skeletal muscles showed similar relationships.

Blood Flow Analysis

All measured organ blood flows, except for the kidney, tended to decrease after rhIL-6 treatment. This was also observed for the gastrocnemius muscle (control, 0.12 ± 0.05 mL · min^{-1} · g^{-1}; moderate dose, 0.10 ± 0.05 mL · min^{-1} · g^{-1}; and high dose, 0.08 ± 0.02 mL · min^{-1} · g^{-1}). However, this tendency reached statistical significance only for the diaphragm (Figure 5) and jejunum (control, 1.89 ± 0.51 mL · min^{-1} · g^{-1}; moderate dose, 1.33 ± 0.47 mL · min^{-1} · g^{-1}; and high dose, 1.10 ± 0.24 mL · min^{-1} · g^{-1}; $P=0.021$).

Heart Histology

Microscopic examination of diastolic right ventricular cavity dimensions revealed significant dose-dependent

TABLE 2. Hemodynamic Variables

	Control	Moderate	High	ANOVA *P*
Steady state				
Heart rate, bpm	435±18	421±54	427±46	0.8
End-systolic volume, μL	42.9±11.7	70.0±13.9†	74.3±24.3‡	<0.005
End-diastolic volume, μL	77.6±12.1	123.2±11.8§	137.3±22.9§	<0.001
End-systolic pressure, mm Hg	113.0±26.6	86.5±17.0*	90.1±16.4*	<0.05
End-diastolic pressure, mm Hg	1.6±1.5	1.9±0.7	2.9±1.4	0.1
Stroke volume, μL	50.1±4.5	79.7±15.3†	87.5±28.7§	<0.005
Ejection fraction, %	58.5±6.7	58.7±9.9	58.4±13.9	1.0
Cardiac output, μL/min	21 866±2451	33 375±6765†	37 070±11 376§	<0.005
Stroke work, mm Hg · μL	4191±716	5593±1571	6494±1601‡	<0.01
Arterial elastance, mm Hg/μL	2.4±0.7	1.2±0.3§	1.2±0.5§	<0.001
dP/dt max, mm Hg/s	7834±2400	6147±1784	7072±2377	0.4
dP/dt min, mm Hg/s	−9066±2729	−6548±2283	−7074±2274	0.1
τ, ms	6.8±0.8	6.9±1.0	7.1±1.2	0.8
Occlusions				
End-systolic elastance, mm Hg/μL	1.8±0.6	0.9±0.7†	0.4±0.1§	<0.001
Preload recruitable stroke work, mm Hg	79.3±14.2	66.9±7.7‖	48.4±11.3§	<0.001
End-diastolic pressure-volume relation slope, mm Hg/μL	0.04±0.02	0.14±0.30	0.03±0.01	0.4

Scheffé post hoc test: *$P<0.094$, †$P<0.05$, ‡$P<0.01$, and §$P<0.005$ vs control; ‖$P=0.016$ vs high dose.

increases in surface when compared with those of control rats (15.4±3.4 μm^2 in controls versus 28.6±5.2 μm^2 in the moderate-dose and 31.9±8.1 μm^2 in the high-dose groups; $P<0.01$; Figure 6).

Lung Histology and Water Content

Left lung microscopic sections of treated animals all showed congestion and interstitial edema, whereas alveolar edema was seen in only some sections (Figure 7). Neither alveolar septal thickening nor focal edema was present in control rats. There were no signs of inflammatory infiltrates in any of the 3 groups. The wet-to-dry ratio of the right lung was significantly higher in moderate- (4.6±0.10) and high- (4.5±0.05) dose groups than in controls (4.2±0.13, $P<0.001$).

Serum Levels

rhIL-6 serum levels averaged 765±529 pg/mL in the moderate-dose group and 12±10 ng/mL in the high-dose group. Conversely, endogenous IL-6 concentrations did not differ among groups and were negligible (mean value of 23±53 pg/mL).

Food Intake

Food intake decreased in all groups immediately after pump implantation (control, −26%; moderate dose, −53%; and high dose, −45%; $P<0.001$). However, at day 1, food intake started to increase in all groups, still yielding a significantly smaller food intake in both treated groups ($P<0.005$). Conversely, from day 5 onward, food intake increased more in

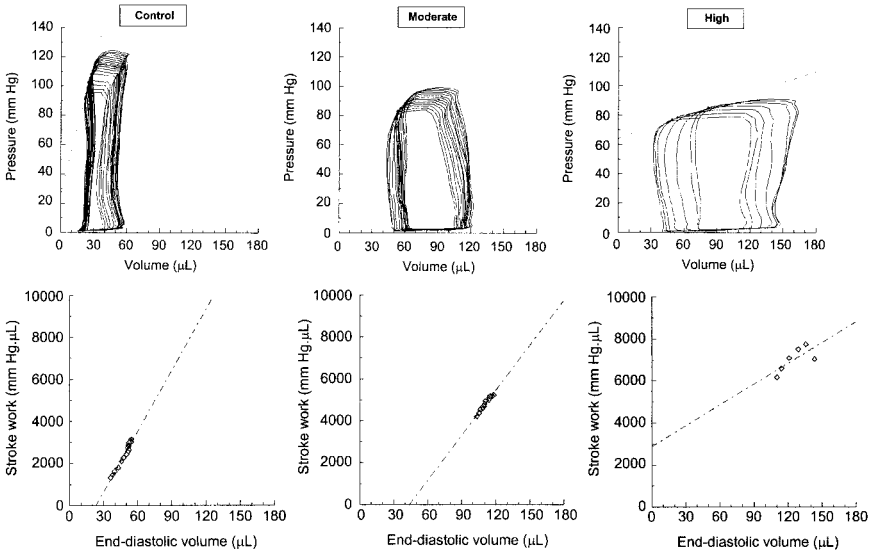

Figure 4. Pressure-volume (top) and stroke work–volume (bottom) relations of left ventricle in control (left), moderate- (middle), and high- (right) dose rhIL-6 groups in 3 representative animals. Pressure is expressed in mm Hg, volume in μL, and stroke work in mm Hg · μL. Dashed line in top panels corresponds to end-systolic pressure–volume relation of left ventricle. Slope of this line denotes end-systolic elastance. In bottom panels, slope corresponds to preload recruitable stroke work. Note dose-dependent decrease in end-systolic elastance, increase in end-diastolic volume, and decrease in preload recruitable stroke work after IL-6 administration. Abbreviations are as defined in text.

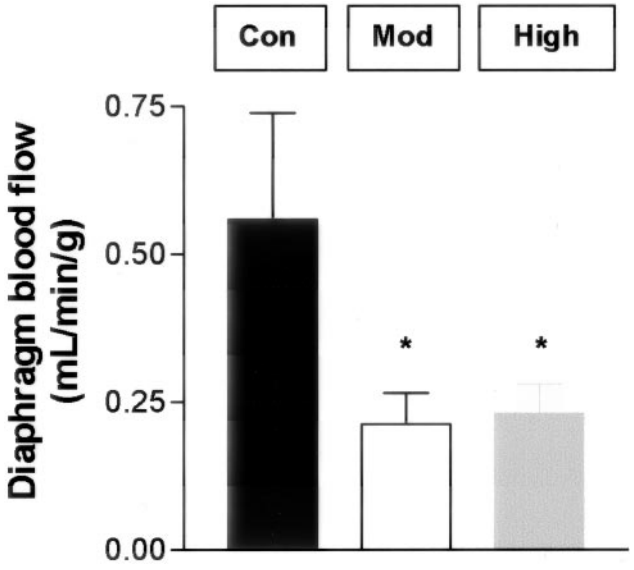

Figure 5. Diaphragm blood flow, expressed in mL · min^{-1} · g^{-1}, in control (Con) rats (solid bar) or rats treated with moderate (Mod; open bar) or high (gray bar) doses of rhIL-6. *$P<0.05$. Abbreviations are as defined in text.

treated rats, so that by the end of treatment, food intake was again similar among all groups (control, 26.10±7.21 g; moderate dose, 25.92±2.65 g; and high dose, 22.88±2.68 g). Body weight decreased significantly after pump implantation in the high-dose group until the end of treatment (control, 412±27 g; moderate dose, 398±20 g; and high dose, 382±10 g; $P<0.05$).

Activity Level

Displacement distance was similar between treated and control rats, both during the day (control, 1286±451 cm/h; moderate dose, 1063±414 cm/h; and high dose, 1165±314 cm/h) and the night (control, 710±521 cm/h; moderate dose, 537±363 cm/h; and high dose, 541±256 cm/h).

Discussion

The present data show that 7-day administration of rhIL-6 to rats resulted in a dose-dependent respiratory and peripheral skeletal muscle atrophy without alterations in diaphragm contractile properties. It also caused a dose-dependent myocardial contractile deterioration, as was evident from alterations in invasive cardiovascular functional parameters, increased lung wet-to-dry ratios, and lung microscopic examination. It appears likely that the observed diaphragm and peripheral muscle atrophy predominantly resulted from blood flow redistribution, because a direct effect of rhIL-6 on the diaphragm was absent.

In the present study, contractility was expressed in grams per square centimeter, meaning that all generated forces were corrected for potential reductions in CSA. Because the observed diaphragm atrophy occurred with unchanged contractile properties, there was, in essence, less muscle with the quality of the remaining muscle unchanged. However, the diaphragm's absolute force generation is expected to be reduced proportionately with respect to reductions in diaphragm weight.

The effects of IL-6 on myocardial function have been well documented in vitro. Reversible negative inotropic effects on isolated hamster papillary muscles,[20] downregulation of SERCA2 in neonatal rat ventricular myocytes,[21] reduced RNA expression of both cardiac myosin heavy chain isoforms, and a loss of cardiac actin in rat cardiac myocytes[22] have been reported. Conversely, although in vivo experiments showed that IL-6 overexpression in mice caused

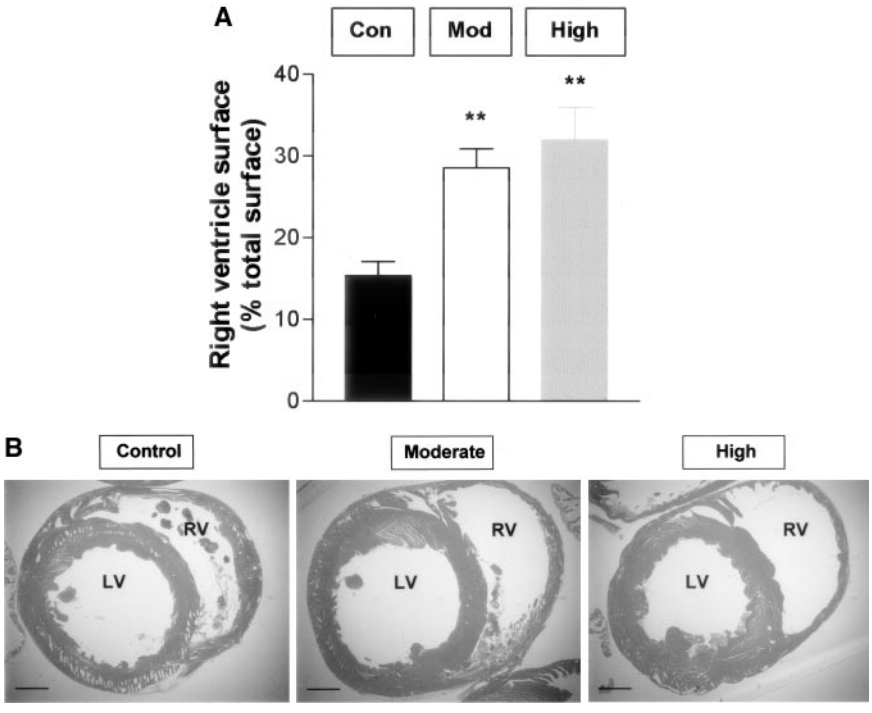

Figure 6. A, Right ventricle surface, expressed as percentage of total heart surface in control (Con) rats (solid bar) or rats treated with moderate (Mod; open bar) or high (gray bar) doses of rhIL-6. **$P<0.01$. B, Heart H&E staining of representative control (left), moderate-dose (middle), and high-dose (right) rhIL-6–treated animals. Panels correspond to ×8 magnification, bar=875 μm. Note dose-dependent dilatation of right ventricular (RV) cavity surface in both treated groups when expressed as percentage of total surface. Left ventricular (LV) dilatation did not occur. Other abbreviations are as defined in text.

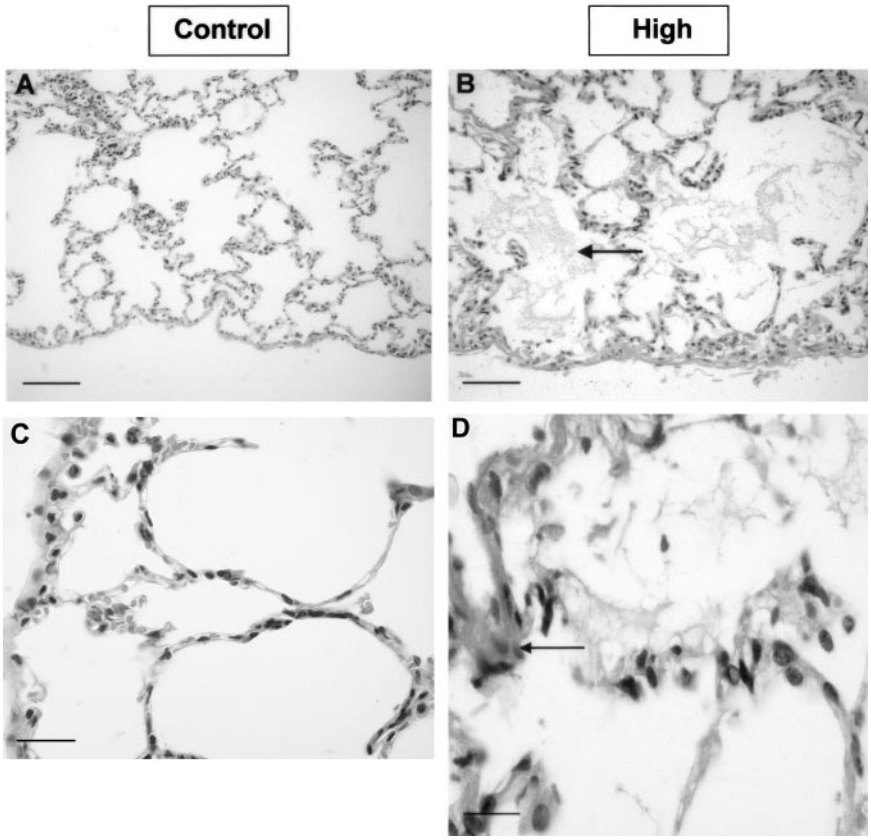

Figure 7. Left lung H&E staining of representative control (left) and high-dose rhIL-6–treated (right) animals. Top panels correspond to ×200 magnification, bar=50 μm; bottom panels, to ×650 magnification, bar=15 μm. Note alveolar edema, identified as pale eosinophilic fluid within groups of alveoli (arrow in B), and congestion or interstitial edema, marked by thickened septa engorged by red blood cells (arrow in D), in micrographs from high-dose group. None of these characteristics were present in control rats. Abbreviations are as defined in text.

skeletal muscle atrophy, a direct negative effect of IL-6 on skeletal muscle cells had never been observed.[12,13]

There is abundant evidence that cardiac failure induces ventilatory and peripheral skeletal muscle atrophy. However, in studies concurrently addressing peripheral and respiratory muscle strength in heart failure patients, the impairment in respiratory muscle contractility was proportionally greater[28–30] or existed even in the absence of peripheral muscle dysfunction.[29] Ventricular dysfunction induced by experimental coronary ligation in rats confirmed the aforementioned findings; ie, moderate ventricular dysfunction affected the diaphragm only, whereas severe heart failure also affected other respiratory and peripheral muscles.[6]

It appears plausible from the present study that skeletal muscle atrophy results from the observed cardiac failure induced by rhIL-6, because the pattern of muscle atrophy observed in the present study was similar to that observed in studies of myocardial failure.[31,32] Furthermore, systolic ventricular dysfunction in rats in which alterations in hemodynamic variables resulted in a pattern of heart failure similar to that in the present study led to an identical pattern of muscle atrophy, also without changes in diaphragm contractile properties.[6] Finally, in the present study, reductions in ventilatory and peripheral muscle weight were related to reduced myocardial contractility.

Other factors might be implicated in the observed skeletal muscle atrophy but probably contributed to a lesser extent. Indeed, short-term nutritional deprivation would be expected to result in selective type IIx/b atrophy in the diaphragm,[33] which is in contrast with the generalized atrophy observed herein. Furthermore, deconditioning was unlikely to be responsible as well, because activity levels were similar among all groups. A direct effect of rhIL-6 to the diaphragm could also be excluded, because no changes in diaphragmatic contractility were observed after in vitro rhIL-6 administration. Conversely, skeletal muscle insulin resistance could not be ruled out in our study and might have contributed somewhat to the observed skeletal muscle atrophy, because it is known that IL-6 administration in mice results in hepatic insulin resistance by inhibiting the insulin-dependent insulin receptor signal transduction at serum concentrations of 112 pg/mL. However, at that concentration, it did not affect the signal transduction pathway in skeletal muscles.[34]

The pattern of hemodynamic alterations observed in the present study is remarkable. Indeed, a dose-dependent heart dilatation was observed, as was evident from increases in end-diastolic volume (moderate dose, 59%; high dose, 77%), leading to functioning at lower end-systolic pressures (−23% and −20%, respectively). Significantly higher stroke volumes (59% and 75%) are compatible with unaltered ejection fraction. However, load-independent contractility parameters decreased significantly; eg, preload recruitable stroke work decreased in a dose-dependent fashion (−16% and −39%). Because peripheral resistance decreased, stroke volume and cardiac output increased despite the reduced cardiac contractility. Although paradoxical at first, this phenomenon was associated with reductions in diaphragm blood flow of ≈60% in both treated groups. In addition, decreases in systolic arterial pressure as observed in the present study are known to decrease diaphragmatic blood flow.[35] This decrease is likely

to be responsible for the diaphragm atrophy observed. A similar trend was present for blood flow to peripheral muscles, though less pronounced. This finding is consistent with the fact that only a tendency to atrophy was observed in the gastrocnemius. Nevertheless, because blood flow reductions were also observed in all measured organs except kidneys, increases in other tissues are expected.

All of these hemodynamic changes do not contradict previous findings showing that IL-6 double-transgenic mice suffered from myocyte hypertrophy and decreases in left ventricular volume.[16] In the latter study, hIL-6 serum levels averaged 0.1 to 5 ng/mL, which was less than observed in our high-dose-group of rats (12.1 ng/mL). This low IL-6 concentration might produce hypertrophy, whereas higher concentrations (as in our study) might further affect the myocardium and produce dilatation, which was especially pronounced in the high-dose group. However, transgenic models are not fully comparable because of overexpression during prenatal and postnatal development, which certainly influences long-term morphological findings such as ventricular hypertrophy and remodeling. Furthermore, cardiotrophin-1 administration, at lower doses than those used in our study, also induced myocyte hypertrophy,[17] decreases in mean arterial pressure, and decreases in systemic vascular resistance without changes in left ventricular maximal *dP/dt*.[18] Those observations are consistent with our results.

The present data may be very clinically significant, because the rhIL-6 serum levels that produced effects in the present study are within the range of those obtained in patients. Even if rats are less susceptible to IL-6 than humans, as demonstrated in human toxicity experiments,[36] a serum level of 12 ng/mL was observed with a dose of 250 $\mu g \cdot kg^{-1} \cdot d^{-1}$. At 100 $\mu g \cdot kg^{-1} \cdot d^{-1}$, at which heart failure was already evident and discrete muscle atrophy was present, a serum level of 765 pg/mL was observed. Both values are in the range of individual serum levels found in patients with sepsis, acute respiratory distress syndrome, and pneumonia.[2,4] Also, in patients suffering from left ventricular dysfunction[1] or after reperfusion of the ischemic heart in cardiopulmonary bypass,[37] IL-6 serum levels are known to be elevated. This may consequently lead to further deterioration of cardiac function, because IL-6 is known to be an independent predictor for worsening of heart failure in patients with end-stage heart failure.[38] Therefore, anticytokine strategies may be useful during cardiac surgery to improve clinical outcomes, as already shown by the beneficial effects of tumor necrosis factor-α and IL-6 removal through hemofiltration in children undergoing cardiopulmonary bypass.[39] Although IL-6 serum levels in heart failure patients are not in the range of those observed in the present study,[1] supranormal levels of rhIL-6 as observed herein are clearly relevant to patients with acute respiratory distress syndrome, pneumonia, and sepsis, in which the same pattern of myocardial failure occurs.[40]

We conclude that 7 days of exogenous administration of rhIL-6 to rats caused dose-dependent skeletal muscle atrophy induced by myocardial failure. These effects occurred at serum levels that are likely to be attained in patients. This may be of major clinical relevance to patients with acute respiratory distress syndrome, pneumonia, or sepsis or those undergoing cardiopulmonary bypass.

Acknowledgments

This study was supported by the Fonds voor Wetenschappelijk Onderzoek-Vlaanderen (FWO), Belgium, grant No. G.0237.01, and FWO Levenslijn grant No. 7.0007.00. Ghislaine Gayan-Ramirez is a postdoctoral fellow of the Fonds voor Wetenschappelijk Onderzoek-Vlaanderen. An Van Den Bergh is a researcher funded by a PhD grant of the Institute for the Promotion of Innovation Through Science and Technology in Flanders (IWT-Vlaaderen). The authors sincerely acknowledge Dr Ahmad Kasran for the serum analyses, Leen Luyts for technical assistance, Veerle Leunens for the microsphere analysis, and Toon Leroy for measuring activity levels. The authors also thank Prof Raf Sciot for preparing the histological slides and Kris Van Kuyck and Veerle Reynders for performing the pilot study. Finally, the authors are grateful to the company Ajinomoto (Japan) and particularly Dr Okano for providing the rhIL-6.

References

1. TorreAmione G, Kapadia S, Benedict C, Oral H, Young JB, Mann DL. Proinflammatory cytokine levels in patients with depressed left ventricular ejection fraction: a report from the studies of left ventricular dysfunction (SOLVD). *J Am Coll Cardiol*. 1996;27:1201–1206.
2. Kragsbjerg P, Holmberg H, Vikerfors T. Dynamics of blood cytokine concentrations in patients with bacteremic infections. *Scand J Infect Dis*. 1996;28:391–398.
3. Yamada Y, Endo S, Inada K. Plasma cytokine levels in patients with severe burn injury: with reference to the relationship between infection and prognosis. *Burns*. 1996;22:587–593.
4. Schutte H, Lohmeyer J, Rosseau S, Ziegler S, Siebert C, Kielisch H, Pralle H, Grimminger F, Morr H, Seeger W. Bronchoalveolar and systemic cytokine profiles in patients with ARDS, severe pneumonia and cardiogenic pulmonary oedema. *Eur Respir J*. 1996;9:1858–1867.
5. Wedzicha JA, Seemungal TA, MacCallum PK, Paul EA, Donaldson GC, Bhowmik A, Jeffries DJ, Meade TW. Acute exacerbations of chronic obstructive pulmonary disease are accompanied by elevations of plasma fibrinogen and serum IL-6 levels. *Thromb Haemost*. 2000;84:210–215.
6. Stassijns G, Gayan-Ramirez G, De Leyn P, Verhoeven G, Herijgers P, de Bock V, Dom R, Lysens R, Decramer M. Systolic ventricular dysfunction causes selective diaphragm atrophy in rats. *Am J Respir Crit Care Med*. 1998;158:1963–1967.
7. Vassilakopoulos T, Zakynthinos E, Roussos C, Zakynthinos S. Respiratory muscles in heart failure. *Monaldi Arch Chest Dis*. 1999;54:150–153.
8. Bolton CF. Sepsis and the systemic inflammatory response syndrome: neuromuscular manifestations. *Crit Care Med*. 1996;24:1408–1416.
9. Yasuhara S, Kanakubo E, Perez ME, Kaneki M, Fujita T, Okamoto T, Martyn JA. The 1999 Moyer Award: burn injury induces skeletal muscle apoptosis and the activation of caspase pathways in rats. *J Burn Care Rehabil*. 1999;20:462–470.
10. American Thoracic Society/European Respiratory Society. Skeletal muscle dysfunction in chronic obstructive pulmonary disease. *Am J Respir Crit Care Med.* 1999;159:S1–S40.
11. Herridge MS, Cheung AM, Tansey CM, Matte-Martyn A, Diaz-Granados N, Al Saidi F, Cooper AB, Guest CB, Mazer CD, Mehta S, Stewart TE, Barr A, Cook D, Slutsky AS. One-year outcomes in survivors of the acute respiratory distress syndrome. *N Engl J Med*. 2003;348:683–693.
12. Fujita J, Tsujinaka T, Ebisui C, Yano M, Shiozaki H, Katsume A, Ohsugi Y, Monden M. Role of interleukin-6 in skeletal muscle protein breakdown and cathepsin activity in vivo. *Eur Surg Res*. 1996;28:361–366.
13. Tsujinaka T, Fujita J, Ebisui C, Yano M, Kominami E, Suzuki K, Tanaka K, Katsume A, Ohsugi Y, Shiozaki H, Monden M. Interleukin 6 receptor antibody inhibits muscle atrophy and modulates proteolytic systems in interleukin 6 transgenic mice. *J Clin Invest*. 1996;97:244–249.
14. Goodman MN. Interleukin-6 induces skeletal muscle protein breakdown in rats. *Proc Soc Exp Biol Med*. 1994;205:182–185.
15. Okazaki S, Kawai H, Arii Y, Yamaguchi H, Saito S. Effects of calcitonin gene-related peptide and interleukin 6 on myoblast differentiation. *Cell Prolif*. 1996;29:173–182.
16. Hirota H, Yoshida K, Kishimoto T, Taga T. Continuous activation of gp130, a signal-transducing receptor component for interleukin 6-related

cytokines, causes myocardial hypertrophy in mice. *Proc Natl Acad Sci U S A*. 1995;92:4862–4866.
17. Jin H, Yang R, Keller GA, Ryan A, Ko A, Finkle D, Swanson TA, Li W, Pennica D, Wood WI, Paoni NF. In vivo effects of cardiotrophin-1. *Cytokine*. 1996;8:920–926.
18. Jin H, Yang R, Ko A, Pennica D, Wood WI, Paoni NF. Effects of cardiotrophin-1 on haemodynamics and cardiac function in conscious rats. *Cytokine*. 1998;10:19–25.
19. Pennica D, King KL, Shaw KJ, Luis E, Rullamas J, Luoh SM, Darbonne WC, Knutzon DS, Yen R, Chien KR. Expression cloning of cardiotrophin 1, a cytokine that induces cardiac myocyte hypertrophy. *Proc Natl Acad Sci U S A*. 1995;92:1142–1146.
20. Finkel MS, Oddis CV, Jacob TD, Watkins SC, Hattler BG, Simmons RL. Negative inotropic effects of cytokines on the heart mediated by nitric oxide. *Science*. 1992;257:387–389.
21. Villegas S, Villarreal FJ, Dillmann WH. Leukemia inhibitory factor and interleukin-6 downregulate sarcoplasmic reticulum Ca^{2+} ATPase (SERCA2) in cardiac myocytes. *Basic Res Cardiol*. 2000;95:47–54.
22. Patten M, Kramer E, Bunemann J, Wenck C, Thoenes M, Wieland T, Long C. Endotoxin and cytokines alter contractile protein expression in cardiac myocytes in vivo. *Pflügers Arch*. 2001;442:920–927.
23. Dekhuijzen PN, Gayan-Ramirez G, de Bock V, Dom R, Decramer M. Triamcinolone and prednisolone affect contractile properties and histopathology of rat diaphragm differently. *J Clin Invest*. 1993;92:1534–1542.
24. Moore BJ, Miller MJ, Feldman HA, Reid MB. Diaphragm atrophy and weakness in cortisone-treated rats. *J Appl Physiol*. 1989;67:2420–2426.
25. Dubowitz V. *Muscle Biopsy: A Practical Approach*. London, England: Balliere Tindall; 1985.
26. Herijgers P, Leunens V, Tjandra-Maga TB, Mubagwa K, Flameng W. Changes in organ perfusion after brain death in the rat and its relation to circulating catecholamines. *Transplantation*. 1996;62:330–335.
27. Bloemen H, Aerts JM, Berckmans D, Goedseels V. Image analysis to measure activity index of animals. *Equine Vet J Suppl*. 1997;23:16–19.
28. Lindsay DC, Lovegrove CA, Dunn MJ, Bennett JG, Pepper JR, Yacoub MH, Poole-Wilson PA. Histological abnormalities of muscle from limb, thorax and diaphragm in chronic heart failure. *Eur Heart J*. 1996;17:1239–1250.
29. McParland C, Resch EF, Krishnan B, Wang Y, Cujec B, Gallagher CG. Inspiratory muscle weakness in chronic heart failure: role of nutrition and electrolyte status and systemic myopathy. *Am J Respir Crit Care Med*. 1995;151:1101–1107.
30. Hammond MD, Bauer KA, Sharp JT, Rocha RD. Respiratory muscle strength in congestive heart failure. *Chest*. 1990;98:1091–1094.
31. Howell S, Maarek JM, Fournier M, Sullivan K, Zhan WZ, Sieck GC. Congestive heart failure: differential adaptation of the diaphragm and latissimus dorsi. *J Appl Physiol*. 1995;79:389–397.
32. Lipkin DP, Jones DA, Round JM, Poole-Wilson PA. Abnormalities of skeletal muscle in patients with chronic heart failure. *Int J Cardiol*. 1988;18:187–195.
33. Nava S, Gayan-Ramirez G, Rollier H, Bisschop A, Dom R, de Bock V, Decramer M. Effects of acute steroid administration on ventilatory and peripheral muscles in rats. *Am J Respir Crit Care Med*. 1996;153:1888–1896.
34. Klover PJ, Zimmers TA, Koniaris LG, Mooney RA. Chronic exposure to interleukin-6 causes hepatic insulin resistance in mice. *Diabetes*. 2003;52:2784–2789.
35. Hussain SN, Roussos C, Magder S. Effects of tension, duty cycle, and arterial pressure on diaphragmatic blood flow in dogs. *J Appl Physiol*. 1989;66:968–976.
36. Olencki T, Finke J, Tubbs R, Elson P, McLain D, Herzog P, Budd GT, Gunn H, Bukowski RM. Phase 1 trial of subcutaneous IL-6 in patients with refractory cancer: clinical and biologic effects. *J Immunother*. 2000;23:549–556.
37. Roth-Isigkeit A, Hasselbach L, Ocklitz E, Bruckner S, Ros A, Gehring H, Schmucker P, Rink L, Seyfarth M. Inter-individual differences in cytokine release in patients undergoing cardiac surgery with cardiopulmonary bypass. *Clin Exp Immunol*. 2001;125:80–88.
38. Gwechenberger M, Hulsmann M, Berger R, Graf S, Springer C, Stanek B, Pacher R. Interleukin-6 and B-type natriuretic peptide are independent predictors for worsening of heart failure in patients with progressive congestive heart failure. *J Heart Lung Transplant*. 2004;23:839–844.
39. Millar AB, Armstrong L, van der Linden J, Moat N, Ekroth R, Westwick J, Scallan M, Lincoln C. Cytokine production and hemofiltration in children undergoing cardiopulmonary bypass. *Ann Thorac Surg*. 1993;56:1499–1502.
40. Metrangolo L, Fiorillo M, Friedman G, Silance PG, Kahn RJ, Novelli GP, Vincent JL. Early hemodynamic course of septic shock. *Crit Care Med*. 1995;23:1971–1975.